Inhalation Toxicology, 2010; 22(12): 1032–1037

informa
healthcare

REVIEW ARTICLE

Inhaled aerosol particle dosimetry in mice: A review

Loyda B. Méndez[1,2], Glenn Gookin[3], and Robert F. Phalen[3]

[1]*Department of Microbiology and Molecular Genetics, School of Biological Sciences, University of California, Irvine, CA, USA,* [2]*Pacific Southwest Regional Center of Excellence, University of California, Irvine, CA, USA, and* [3]*Department of Medicine, School of Medicine, University of California, Irvine, CA, USA*

Abstract
The availability of molecular and genetic tools has made the mouse the most common animal model for a variety of human diseases in toxicology studies. However, little is known about the factors that will influence the dose delivery to murine lungs during an inhalation study. Among these factors are the respiratory tract anatomy, lung physiology, and clearance characteristics. Therefore, the objective of this paper is to briefly review the current knowledge on the aforementioned factors in mice and their implications to the dose delivered to mouse models during inhalation studies. Representative scientific publications were chosen from searches using the NCBI PubMed and ISI Web of Knowledge databases. Relevant respiratory physiological differences have been widely reported for different mouse strains and sexes. The limited data on anatomical morphometry that is available for the murine respiratory tract indicates significant differences between mouse strains. These differences have implications to the dose delivered and the biological outcomes of inhalation studies.

Keywords: *Aerosol; inhalation studies; dosimetry; respiratory tract; mouse*

Introduction

Inhalation studies with mice hold the promise of better understanding the effects of air pollutants on compromised human populations. However, little is known about the factors that will influence dose delivery into the lungs of murine models during an inhalation study. Among the important factors are the respiratory tract anatomy, lung physiology, and particle clearance characteristics. Morphometric studies using mice are rare, but they have found significant differences in the airway morphometry of two murine strains with different genetic backgrounds (Oldham et al., 1994; Oldham and Robinson, 2007). Relevant differences in respiratory physiology have also been reported for different mouse strains and sexes (Tankersley et al., 1994; Reinhard et al., 2002; Flandre et al., 2003). In addition, structural and physiological alterations in mouse models of susceptibility as well as in genetically engineered mice may significantly influence inhaled particle deposition (Mall, 2008). These differences have implications to the dose delivered and the biological outcomes of inhalation studies. Therefore, the objective of this paper is to review the current state of knowledge regarding inhalation dosimetry for mice. Information was obtained from the scientific literature (e.g. using NCBI PubMed and ISI Web of Knowledge) as well as data obtained in our laboratory.

Dosimetry considerations

A fundamental requirement in a toxicology study is that the dose delivered be known. However in inhalation toxicology, the dose is often expressed in terms of exposure due to difficulties in measuring the actual inhaled deposition dose during an experiment. Therefore, inhaled particle doses must often have to be estimated using mathematical relationships in order to interpret experimental results. Dosimetry techniques can establish the relationship between exposure and the doses delivered to and retained by target sites. Deposition, clearance, translocation, and retention comprise the essential elements of dosimetry (US EPA, 2009).

The initial aerosol deposition dose for inhaled particles of a distinct size can be defined as the product of the aerosol concentration in the breathing zone, the exposure duration, the subject's ventilation rate, the sampling

Address for Correspondence: Loyda B. Mendez, Department of Microbiology and Molecular Genetics, Pacific Southwest Regional Center of Excellence, University of California, Irvine, CA 92697-4028, USA. E-mail: mendezl@uci.edu

(Received 16 June 2010; revised 10 August 2010; accepted 11 August 2010)

ISSN 0895-8378 print/ISSN 1091-7691 online © 2010 Informa Healthcare USA, Inc.
DOI: 10.3109/08958378.2010.515624
http://www.informahealthcare.com/iht

efficiency or inhalability, and the deposition efficiency. This dose represents the total initial aerosol dose delivered and deposited in the respiratory tract since particle clearance and sites of local deposition within the respiratory tract are not included. The initial inhaled dose is often normalized to body weight, but it may be also normalized to a distinct property of the biological target, such as tissue mass, surface area, or volume. In spite of its limitations, this initial dose is most often used to correlate with the biological effects in a toxicology study, and to perform extrapolation calculations (Jarabek et al., 2005).

The biological activity of an inhaled particle can be influenced by the exposure modality (e.g. nose only vs. whole body), the aerosol characteristics (e.g. chemistry, size, and shape), the sites of deposition in the respiratory tract, the animal species, and even specific strains under study. In turn, aerosol deposition in different regions of the respiratory tract depends on particle characteristics, lung morphology, tidal volume, and breathing rate. For the purpose of this paper we will provide an overview of several anatomical and physiological factors that affect aerosol doses in mouse models. In addition, we will briefly review the dosimetric mathematical models that are currently available for the mouse.

Aerosol deposition phenomena

Inhaled particles will deposit in the respiratory tract if they move out of the air streams to come in contact with an airway surface. Although many mechanisms influence particle deposition, three main mechanisms that are usually included in mathematical dosimetry models are: inertial impaction; gravitational sedimentation; and Brownian diffusion (ICRP, 1994; NCRP, 1997; Brown et al., 2005). These deposition mechanisms are independent of the animal species, but their relative importance is not. The deposition efficiency of particles in the different subregions of the respiratory tract (e.g. extrathoracic (ET), tracheobronchial (TB), and pulmonary (P)) will be dependent on the aerosol characteristics, delivery system used, breathing patterns, and airway morphology. The probability of particle deposition due to impaction is a function of the local airflow velocity, airway geometry, and particle inertia. Inertial impaction is an efficient deposition mechanism in areas with sharp transitions, as occur in the nasal turbinates, larynx, and at airway bifurcations. The probability for particle deposition due to sedimentation is proportional to residence time in the airways, particle size and density, and inversely proportional to breathing frequency. The probability for particles smaller than about 0.2 μm in diameter to deposit in the respiratory tract due to diffusion is proportional to residence time in the airways and is greater in areas of low airflow velocity and areas with turbulent flow (Housiadas and Lazaridis, 2010). Even minor anatomical differences, as occur in strains within species, have the potential to significantly alter the total and local deposition efficiencies of inhaled aerosol particles.

Respiratory tract physiology

Physiological factors including breathing patterns and clearance mechanisms influence total and regional sites of particle doses. Among the breathing pattern phenomena that influence inhaled particle deposition are frequency, tidal volume, and minute ventilation. The more air that is inspired per unit time will directly increase the initial inhaled particle dose. Small animals, such as mice, inhale greater volumes of air normalized to body mass than their larger counterparts. The tidal volume and dead space volume affect deposition by influencing the depth of penetration of inspired air. The respiratory frequency and the duration of respiratory pauses will influence particle deposition due to sedimentation and diffusion mechanisms by affecting particle residence time in the respiratory tract. In addition, inspiratory and expiratory airflow rates will influence particle deposition efficiency throughout the respiratory tract. It is important to note that differences in breathing parameters among mouse strains and varieties have been widely reported in the literature (Tankersley et al., 1994, 1997; Han and Strohl; 2000, Schulz et al., 2002; Flandre et al., 2003). Table 1 shows respiratory frequencies (f), tidal volumes (V_t), and respiratory minute ventilation in several mouse strains. Particle clearance within the respiratory tract is dependent on the site of particle deposition. Particle clearance rates and mucociliary transport velocities in the upper respiratory tract (URT) and trachea have been reported for the mouse (Snipes et al., 1983; Brownstein, 1987; Hsieh et al., 1999; Foster et al., 2001; Grubb et al., 2004). Physiological factors in the mouse have been shown to be dependent on many factors, including strain, gender, age, and disease status. In addition, transgenic mice can be designed to alter specific physiological factors that might modify the inhaled, deposited, and retained doses of particles in the respiratory tract (Grubb et al., 2004; Mall, 2008).

Table 1. Reported values of respiratory parameters in mice.

Strain	n	f (min^{-1})	V_t (ml)	RMV (ml·min^{-1})
Method: Unrestrained whole-body plethysmography				
A/J	5*	148.2	0.195	28.85
Balb/c	6*	144.6	0.166	23.87
B6C3F1	14†	180	0.151	27.22
C3H/HeJ	8*	106.2	0.235	24.91
	20†	108	0.249	26.71
C57BL/6	20†	163.2	0.159	25.51
	8*	168.6	0.185	31.15
Method: Restrained whole-body plethysmography				
A/J	18‡	277.9	0.245	67.7
	5¶	352	0.24	84.5
Balb/c	18‡	327	0.210	67.1
	517§	273	0.219	59.73
	5¶	336	0.20	67.2
CD-1	5¶	272	0.24	65.3
C57BL/6	18‡	357.7	0.281	100.3
	381§	302.3	0.225	67.83
B6C3F1	5¶	339	0.23	77.97

*Tankersley et al. (1994); †Tankersley et al. (1997); ‡Lofgren et al. (2006); ¶DeLorme and Moss (2002); §Flandre et al. (2003).

Respiratory tract anatomy

The mammalian respiratory tract can be divided in three main regions: ET, TB, and P). The airway anatomy in these regions is dependent on many factors, including species, strain, body size, frequently gender, and others. Anatomical features in each region can differ significantly among mouse strains and varieties. The respiratory tract geometry affects particle deposition in many ways. For example, airway diameter sets the maximum transverse displacement required for an airborne particle to contact a surface, while the cross-sectional area determines the airflow velocity and type of flow (i.e. laminar, turbulent, or mixed) for a given inspiratory flow rate. Therefore, the quantitative morphometric data available for the mouse respiratory tract will be briefly addressed.

ET region

The ET region, also known as the head airways or URT, extends from the nares down to the entrance of the trachea. The ET region includes the mouth, nasal cavity, pharynx, and larynx. The main mechanisms of particle deposition in the ET region are impaction and diffusion. Enhanced particle deposition in the URT occurs in areas characterized by obstructions (e.g. turbinates), constrictions (e.g. larynx), directional changes (e.g. pharyngeal bend), and high air velocities (e.g. nasal and laryngeal cavities). Although a complete anatomical model of the ET region of the mouse is not available, limited quantitative morphometric data have been reported and/or estimated for different areas of the URT (Gross et al., 1982; Andersen et al., 2000), as shown in Table 2.

The nasal cavity of mice is structurally complex and is the primary site of entry of inhaled air in the respiratory tract, as oral inhalation has not been seen to occur naturally. The nasal airways are divided into two passages by the nasal septum with each passage extending from the nostrils to the nasopharynx. The shape and complexity of the nasal turbinates is important factor in the filtration of inhaled aerosols by the ET region. Other factors influencing particle deposition in the nasal airways include the high volume of airflow through the ventral aspect of the nasal cavity over the nasal and maxillary turbinates and the pressure drop generated by the nasal region (Harkema et al., 2006). Gross et al. (1982) determined the nasal cavity length, and the total surface area and volume for the B6C3F1 mouse (Table 2). Additional quantitative data on the mouse nasal cavity in Table 2 have been taken from other independent studies (e.g. Andersen et al., 2000).

Table 2. URT morphometry data.

	Length (mm)	Surface area (mm^2)	Volume (mm^3)
Measured values*			
Nasal cavity	5.1	289	31.5
Estimated values†			
Nasal vestibule		44.0	2.0
Dorsal respiratory zone		4.0	0.5
Dorsal olfactory zone		134	8.5
Ventral respiratory zone		133	20.0
Nasopharynx		20.0	0.7

*Gross et al. (1982); †Andersen et al. (2000).

The nasal pharynx is defined as the airway posterior to the termination of the soft palate, where the two air streams exiting the nasal cavity merge before entering the larynx and the TB region. The cross-sectional area of the nasal pharynx and its bend angle are important parameters that will affect particle deposition in this area. Limited quantitative data is available for the pharyngeal region of the New Zealand white mouse (Brennick et al., 2009). These investigators found that the dynamic cross-sectional area of the pharyngeal airways of an obese mouse model is significantly smaller than the lean counterpart, which can influence particle deposition in this area and have repercussions for subsequent particle deposition in the larynx, TB, and P region.

The larynx is a bilaterally symmetric organ characterized by its geometrically complex and variable protuberances, pouches, and folds. Its geometry varies with airflow and phonation. The laryngeal airway is a region of airflow acceleration (due to its constriction) that connects the URT to the TB region. The so-called "laryngeal jet" may enhance particle deposition in the trachea. Although detailed histological and anatomical descriptions of the mouse larynx are available in the literature, there is a lack of quantitative morphometric data that can be used to predict particle deposition in this area (Thomas et al., 2009).

TB region

The mammalian TB tree, which includes the trachea down to the terminal bronchioles can be subdivided into the bronchial region, which includes the trachea and main bronchi, and the bronchiolar region which consists of bronchioles and terminal bronchioles (Newton, 1995). The main mechanisms of particle deposition in the TB region are impaction, sedimentation, and diffusion. Therefore, the branching mode and detailed features of airway geometry are important factors influencing the mechanisms and sites of particle deposition in the TB region. Branching angles determine changes in airflow direction at bifurcations, and thus affect particle deposition due to impaction, while the inclination angles relative to gravity affect particle sedimentation mechanisms. Linear dimensions such as the airway length and diameter, along with the number of airway units, at a given branching generation determine the volume and cross-sectional area, which strongly influences the airflow velocity, and establishes the type of flow regimen in the TB airways (e.g. laminar, turbulent, or mixed).

Quantitative morphometric analysis of the mouse TB airway geometry for two mouse strains, the B6C3F1 and the Balb/c, are available in the literature (Oldham et al., 1994; Oldham and Robinson, 2007). Detailed measurements of replica mouse lung casts have provided data for typical-length pathways, airway lengths and diameters, as well as branching and gravity inclination angles (Table 3). Oldham and Robinson (2007) reported a typical-length pathway of 15 generations for the Balb/c mouse. However the number of airway generations from trachea to terminal bronchioles

Table 3. Branch and gravity angles of TB airways measured in two mouse strains (±SE).

Generation number	Branch angle (°)		Gravity angle (°)	
	B6C3F1*	Balb/c†	B6C3F1	Balb/c
1	0±0	0±0	90±0	90±0
2	14±1	14±1	78±3	105±3
3	18±2	25±6	85±7	98±4
4	30±4	26±6	77±3	91±1
5	12±2	18±3	71±6	78±3
6	10±2	18±2	71±4	76±3
7	11±3	12±3	60	60
8	10±0	22±4	60	60
9	16±2	16±3	60	60
10	11±3	9±2	60	60
11	12±1	24±4	60	60
12	18±3	20±3	60	60
13	22±3	16±3	60	60
14	33±6	26±3	60	60
15	61±1	56±3	60	60

*Oldham et al. (1994); †Oldham and Robinson (2007).

can range from 6 to 27, which will have an effect on the intra- and inter-lobar distribution of deposited particles. Significant differences in airway linear dimensions and cross-sectional areas for the two mouse strains are mainly observed in the bronchial region (Figure 1A, 1B, 1C). These differences have a dramatic effect on the TB tree volume (Figure 1D). It is predicted that these strain variations in the TB tree geometry will result in different inhaled doses and possibly different biological outcomes (Moss and Oldham, 2006).

Pulmonary region

The P region of the mouse consists of the alveolar ducts and sacs, as mice lack respiratory bronchioles (Phalen, 2009). The main mechanisms of particle deposition in the P region are sedimentation and diffusion. The number of alveoli and alveolar surface area for the mouse is available in the literature (Mercer et al., 1994; Knust et al., 2009). Quantitative morphometric data for the alveolar size have been reported for different mouse strains as shown in Table 4. Quantitative data

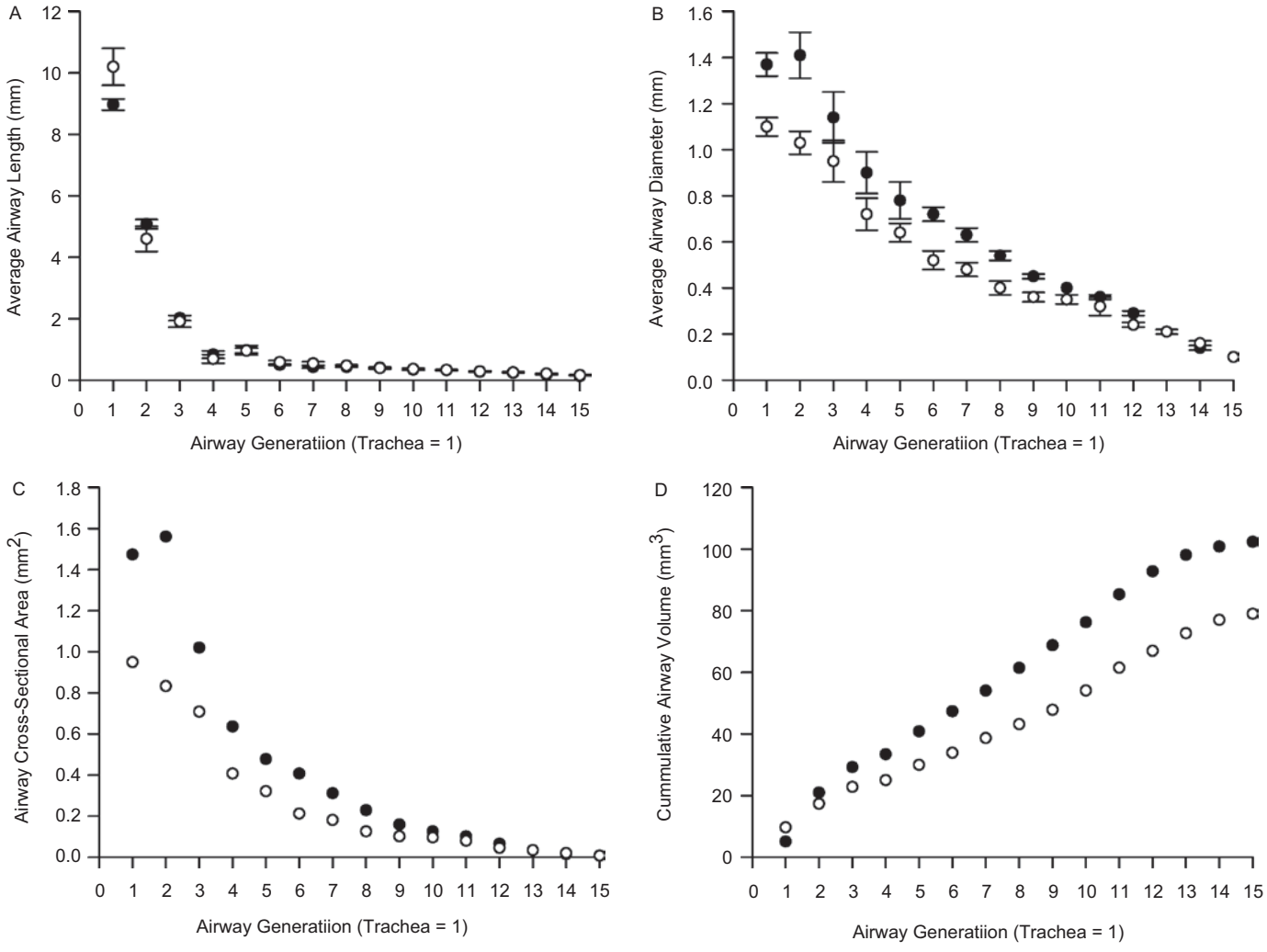

Figure 1. TB region airway dimensions derived from replica rubber lung casts of two mouse strains. (Oldham et al., 1994; Oldham and Robinson, 2007): (A) airway lengths, (B) airway diameters, (C) airway cross-sectional area, and (D) cumulative airway volume. Open circles are B6C3F1 mouse strain and closed circles are for the Balb/c mouse. Error bars are standard error; in some cases the error bars are smaller than the symbols.

for the branching structure beyond the terminal bronchiole has been estimated using the assumptions for rats of Yeh et al. (1979); for two mouse strains (Oldham et al., 1994; Oldham and Robinson, 2007). Differences in alveolar size among inbred mouse strain and for mouse models of lung disease have also been reported (Soutiere et al., 2004; Parameswaran et al., 2009). These structural differences may affect particle deposition due to factors such as variations on the distance between the aerosols and alveolar walls, residence times, and airflow patterns.

Experimental and predicted particle deposition

Experimental nose-only inhalation data

The most complete data to date on total and regional particle deposition in the mouse lung is that published by Raabe et al. (1988) (Table 5). In addition to Raabe's data, other groups have reported deposition fractions for additional (both smaller and larger) particle sizes (Alessandrini et al.; 2008, Thomas et al., 2008). Alessandrini et al. (2008) exposed Balb/c female mice to iridium labeled particles of 35 nm count median diameter and reported a total deposited fraction of 34% with 1% depositing in the ET airways. Of the total respiratory tract deposition, 40% was reported for the combined ET and TB airways, and of 60% for the alveolar region. Thomas et al. (2008) exposed female Balb/c mice to 12.4 μm aerosols, using a large-droplet aerosol generator, containing ~7 microspheres (each 1.1 μm in diameter) per droplet. In this study, the reported deposition fractions were 36.5% in the URT, 0.64% in the trachea, and 1.4% in the deeper region of the lungs.

Mathematical models

Any dosimetry model should first consider the aerosol particle inhalability, which for nasal inhalation, is the sampling efficiency at the entrance of the nares. Although little is known about the inhalability of particles in the mouse, a logistic function for particle inhalability in small laboratory animals have been described based on Raabe's combined data for the mouse, rat, guinea pig, and hamster (Ménache et al., 1995). Inhalability for particles with aerodynamic or physical diameters of about 0.7 μm or less is taken to be >95%; 55% for 7 μm particles; and <45% for 10 μm particles. However these values should only be used with caution in murine dosimetry, as they might be lower for the mouse.

Semi-empirical mathematical models have been established to predict nasal deposition efficiency in the mouse (Phalen and Oldham, 1991; Oldham et al., 1994; US EPA, 1994; Nadithe et al., 2003). These models have been fitted to Raabe's data and mainly predict particle deposition due to impaction as a function of either flow rate or pressure drop. Figure 2 shows the predicted particle deposition for particles with aerodynamic diameters of 0.3–10 μm. However, experimental data is needed to confirm and/or validate these model predictions. Mechanistic models, based on the whole-lung typical pathway reported by Oldham et al. (1994) and Oldham and Robinson (2007) for the B6C3F1 and the Balb/c mouse, have been described to predict particle deposition in the TB region. Since the lung casts used to provide TB morphometry data were assumed to be made at a total lung capacity, Hsieh et al. (1999) and Nadithe et al. (2003) adjusted the values to a functional residual capacity of 0.84 ml. Experimental data appears to agree with model-predicted values of particle deposition in the TB region of mice (Nadithe et al., 2003; Oldham et al., 2009). Mathematical models predicting particle deposition efficiency in the P region are perhaps limited because of the use of unproven assumptions to extrapolate anatomical data for this region (Hsieh et al., 1999; Nadithe et al., 2003; Oldham and Robinson, 2007). Although morphometric data have been reported for alveolar surface area, size and volume, it has not been incorporated in these models.

Table 4. P region morphometry data.

Mouse strain	No. alveoli ($\times 10^6$)	Mean chord length (μm)	Surface area (μm^2)	Volume (μm^3)
Unspecified*	4.20	58	5690	46,900
A/J†		38.8		
C3H/HeJ†		45.3		
C57BL/6†		35.6		
C57BL/6‡	2.31		3620	59,500

*Mercer et al. (1994); †Soutiere et al. (2004); ‡Knust et al. (2009).

Table 5. Deposition fraction (%) of inhaled particles in CF_1 mouse*.

Dae† (μm)	Head	Larynx	Trachea	Bronchial	Pulmonary
0.27	7.68	1.4	0.68	19.91	64.58
1.09	7.26	1.35	0.30	9.97	16.39
3.45	26.74	2.25	0.75	2.14	0.96
4.49	26.90	3.70	0.23	0.89	0.23
5.98	59.10	2.30	0.80	0.60	0.40
9.65	71.50	3.30	0.26	0.40	0.04

*Adapted from Raabe et al. (1988).
†Dae = aerodynamic diameter.

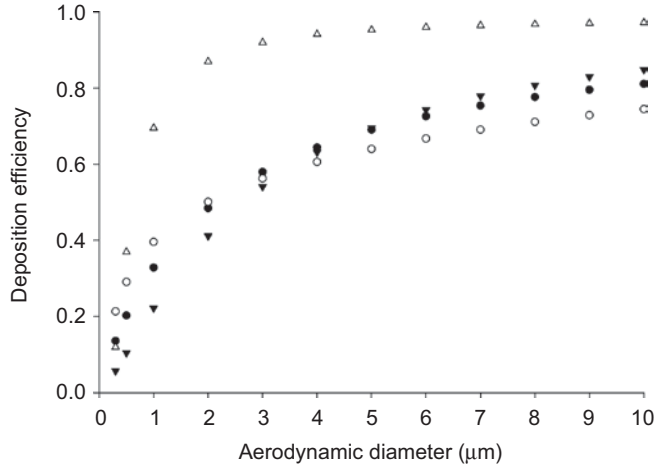

Figure 2. Upper respiratory tract deposition efficiencies calculated according to the equations reported by (•) US EPA (1994), (○) Phalen and Oldham (1991), (▾) Oldham et al. (1994), and (▵) Nadithe et al. (2003).

Conclusions

Although much is known about the variations in respiratory tract anatomy and physiology among mouse strains and varieties, the data are only beginning to elucidate the differences in inhaled particle doses. Additional morphometric information on all of the regions of the respiratory tract is needed before doses in inhalation studies can be predicted. In the meantime, actual deposition determinations should be made in studies as they are performed.

Declaration of interest

This work was supported by NIH Award: AI065359. Additional support was provided by the Charles S. Stocking Family Fund, by way of an endowment to Dr. R.F.P.

References

Alessandrini F, Semmler-Behnke M, Jakob T, Schulz H, Behrendt H, Kreyling W. 2008. Total and regional deposition of ultrafine particles in a mouse model of allergic inflammation of the lung. Inhal Toxicol 20:585–593.

Andersen M, Sarangapani R, Gentry R, Clewell H, Covington T, Frederick CB. 2000. Application of a hybrid CFD-PBPK nasal dosimetry model in an inhalation risk assessment: an example with acrylic acid. Toxicol Sci 57:312–325.

Brennick MJ, Pack AI, Ko K, Kim E, Pickup S, Maislin G, Schwab RJ. 2009. Altered upper airway and soft tissue structures in the New Zealand Obese mouse. Am J Respir Crit Care Med 179:158–169.

Brown JS, Wilson WE, Grant LD. 2005. Dosimetric comparisons of particle deposition and retention in rats and humans. Inhal Toxicol 17: 355–385.

Brownstein DG. 1987. Tracheal mucociliary transport in laboratory mice: evidence for genetic polymorphism. Exp Lung Res 13:185–191.

DeLorme MP, Moss OR. 2002. Pulmonary function assessment by whole-body plethysmography in restrained versus unrestrained mice. J Pharmacol Toxicol Methods 47:1–10.

Flandre TD, Leroy PL, Desmecht DJ. 2003. Effect of somatic growth, strain, and sex on double-chamber plethysmographic respiratory function values in healthy mice. J Appl Physiol 94:1129–1136.

Foster WM, Walters DM, Longphre M, Macri K, Miller LM. 2001. Methodology for the measurement of mucociliary function in the mouse by scintigraphy. J Appl Physiol 90:1111–1117.

Gross EA, Swenberg JA, Fields S, Popp JA. 1982. Comparative morphometry of the nasal cavity in rats and mice. J Anat 135:83–88.

Grubb BR, Jones JH, Boucher RC. 2004. Mucociliary transport determined by *in vivo* microdialysis in the airways of normal and CF mice. Am J Physiol Lung Cell Mol Physiol 286:L588–L595.

Han F, Strohl KP. 2000. Inheritance of ventilatory behavior in rodent models. Respir Physiol 121:247–256.

Harkema JR, Carey SA, Wagner JG. 2006. The nose revisited: a brief review of the comparative structure, function, and toxicologic pathology of the nasal epithelium. Toxicol Pathol 34:252–269.

Housiadas C, Lazaridis M. 2010. Inhalation Dosimetry Modelling. In: Lazaridis M & Colbeck I (eds.) Human Exposure to Pollutants via Dermal Absorption. New York: Springer, 185–236.

Hsieh TH, Yu CP, Oberdörster G. 1999. Deposition and clearance models of Ni compounds in the mouse lung and comparisons with the rat models. Aerosol Sci Technol 5:358–372.

ICRP (International Commission on Radiological Protection). 1994. Human Respiratory Tract Model for Radiological Protection. Publication 66. New York: Pergamon Press.

Jarabek AM, Asgharian B, Miller FJ. 2005. Dosimetric adjustments for interspecies extrapolation of inhaled poorly soluble particles (PSP). Inhal Toxicol 17:317–334.

Knust J, Ochs M, Gundersen HJ, Nyengaard JR. 2009. Stereological estimates of alveolar number and size and capillary length and surface area in mice lungs. Anat Rec (Hoboken) 292:113–122.

Lofgren JL, Mazan MR, Ingenito EP, Lascola K, Seavey M, Walsh A, Hoffman AM. 2006. Restrained whole body plethysmography for measure of strain-specific and allergen induced airway responsiveness in conscious mice. J Appl Physiol 101:1495–1505.

Mall MA. 2008. Role of cilia, mucus, and airway surface liquid in mucociliary dysfunction: lessons from mouse models. J Aerosol Med Pulm Drug Deliv 21:13–24.

Ménache MG, Miller FJ, Raabe OG. 1995. Particle inhalability curves for humans and small laboratory animals. Ann Occup Hyg 39:317–328.

Mercer RR, Russell ML, Crapo JD. 1994. Alveolar septal structure in different species. J Appl Physiol 77:1060–1066.

Moss OR, Oldham MJ. 2006. Dosimetry counts: molecular hypersensitivity may not drive pulmonary hyperresponsiveness. J Aerosol Med 19:555–564.

Nadithe V, Rahamatalla M, Finlay WH, Mercer JR, Samuel J. 2003. Evaluation of nose-only aerosol inhalation chamber and comparison of experimental results with mathematical simulation of aerosol deposition in mouse lungs. J Pharm Sci 92:1066–1076.

NCRP (National Council on Radiation Protection and Measurements). 1997. Deposition Retention and Dosimetry of Inhaled Radioactive Substances. NCRP Report No. 125. Bethesda, MD: National Council on Radiation Protection and Measurements.

Newton PE. 1995. Inhalation Toxicology. *In*: Derelanko MJ & Hollinger MA (eds) CRC Handbook of Toxicology. 1st ed. Boca Raton, FL: CRC Press, 217–276.

Oldham MJ, Phalen RF, Budimen T. 2009. Comparison Of Predicted And Experimentially Measured Aerosol Deposition Efficiency in Balb/C Mice In A New Nose Only System. Aerosol Sci Technol, 43, 970–977.

Oldham MJ, Phalen RF, Schum M, Daniels DS. 1994. Predicted Nasal And Tracheobronchial Particle Deposition Efficiencies for the Mouse. Ann Occup Hygiene, 38, 135–141.

Oldham MJ, Robinson RJ. 2007. Predicted tracheobronchial and pulmonary deposition in a murine asthma model. Anat Rec (Hoboken) 290:1309–1314.

Parameswaran H, Bartolák-Suki E, Hamakawa H, Majumdar A, Allen PG, Suki B. 2009. Three-dimensional measurement of alveolar airspace volumes in normal and emphysematous lungs using micro-CT. J Appl Physiol 107:583–592.

Phalen RF. 2009. Inhalation Studies: Foundations and Techniques, New York, NY, Informa Healthcare.

Phalen RF, Oldham MJ. 1991. An Airway Model for the Laboratory Mouse. Final Research Report submitted to NiPERA, Inc.

Raabe OG, Al-Bayati MA, Teague SV, Rasolt A. 1988. Regional Deposition Of Inhaled Monodisperse Coarse And Fine Aerosol Particles In Small Labratory Animals. Ann Occup Hygiene, 32, 53–63.

Reinhard C, Eder G, Fuchs H, Ziesenis A, Heyder J, Schulz H. 2002. Inbred strain variation in lung function. Mamm Genome 13:429–437.

Schulz H, Johner C, Eder G, Ziesenis A, Reitmeier P, Heyder J, Balling R. 2002. Respiratory mechanics in mice: strain and sex specific differences. Acta Physiol Scand 174:367–375.

Snipes MB, Boecker BB, McClellan RO. 1983. Retention of monodisperse or polydisperse aluminosilicate particles inhaled by dogs, rats, and mice. Toxicol Appl Pharmacol 69:345–362.

Soutiere SE, Tankersley CG, Mitzner W. 2004. Differences in alveolar size in inbred mouse strains. Respir Physiol Neurobiol 140:283–291.

Tankersley CG, Fitzgerald RS, Kleeberger SR. 1994. Differential control of ventilation among inbred strains of mice. Am J Physiol 267:R1371–R1377.

Tankersley CG, Fitzgerald RS, Levitt RC, Mitzner WA, Ewart SL, Kleeberger SR. 1997. Genetic control of differential baseline breathing pattern. J Appl Physiol 82:874–881.

Thomas LB, Stemple JC, Andreatta RD, Andrade FH. 2009. Establishing a new animal model for the study of laryngeal biology and disease: an anatomic study of the mouse larynx. J Speech Lang Hear Res 52:802–811.

Thomas RJ, Webber D, Sellors W, Collinge A, Frost A, Stagg AJ, Bailey SC, Jayasekera PN, Taylor RR, Eley S, Titball RW. 2008. Characterization and deposition of respirable large- and small-particle bioaerosols. Appl Environ Microbiol 74:6437–6443.

US EPA. 1994. Methods for Derivation of Inhalation Reference Concentrations and Application of Inhalation Dosimetry, EPA/600/8-90/066F. U.S. Environmental Protection Agency, Washington, D.C.

US EPA. 2009. Integrated Science Assessment for Particulate Matter, EPA/600/R-08/139F. U.S. Environmental Protection Agency, Washington, D.C.

Yeh HC, Schum GM, Duggan MT. 1979. Anatomic models of the tracheobronchial and pulmonary regions of the rat. Anat Rec 195: 483–492.